Supp. Materials and Methods

International Society for Clinical Electrophysiology of Vision (ISCEV) standard full-field electroretinography (ffERG) was performed using monopolar corneal electrodes (Henkes type; Medical Workshop B.V., Groningen, The Netherlands) and a computerized system (UTAS 3000; LKC, Gaithersburg, MD, USA). Cone responses to 30-Hz flashes of white light were acquired under a background light of 21 cd/m^2. Scotopic responses, including a rod response to a dim blue flash and a mixed cone–rod response to a standard white flash, were acquired after 30-45 minute of dark adaptation. Between 2 and 4 sets of responses were recorded in each condition for reproducibility. All ERG responses were filtered at 0.3 to 500 Hz, and signal averaging was applied. Color fundus photos were obtained using a Zeiss fundus camera (model FF450PLUS; Carl Zeiss Meditec, Dublin, CA, USA). Optical coherence tomography (OCT) imaging was carried out using the Spectralis system (Heidelberg Engineering, Heidelberg, Germany).

Homozygosity mapping was performed on the index case (MOL0339 III:3), the affected brother (MOL0339 III:4), and two unaffected siblings (MOL0339 III:1 and III:2) using Affymetrix (Santa Clara, CA) SNP microarray platform 6.0. Homozygous regions were identified using HomozygosityMapper (http://www.homozygositymapper.org/) (Seelow et al., 2009) and marked by at least 3900 consecutive homozygous SNPs. Homozygous regions were first searched for genes previously associated with retinal phenotype. Whole exome capture was performed using Agilent SureSelect^{XT} Human All Exon V5 Kit (Agilent Technologies, Santa Clara, CA) on 3 μg of fragmented (Covaris, Woburn, MA) genomic DNA, following manufacturer's instructions. Clonal clusters were generated from captured libraries using Illumina Cluster Station. Single-end, 110 bp sequence reads were obtained by Genome Analyzer IIx (Illumina, San Diego, CA).

FastQC (Version 0.10.1; http://www.bioinformatics.babraham.ac.uk/projects/fastqc) quality control tool was utilized to assess quality scores at each individual nucleotide position of sequence reads. Mapping against the human reference genome NCBI build 37 (hg19) was performed using Genomatix Mining Station (Version 0.0.20140128; https://www.genomatix.de/solutions/genomatix-mining-station.html) commercially available next generation sequencing data processing toolkit. Duplicates and non-unique alignments were removed using SAMtools (Versions 0.1.19; http://samtools.sourceforge.net/) (Li et al., 2009),

followed by identification of single nucleotide variants and small insertion-deletions. The variants were annotated using ANNOVAR (last modified 23 August, 2013; http://annovar.openbioinformatics.org/en/latest/) (Wang et al., 2010). Only nonsynonymous variants were considered assuming that potential causal variants would alter the protein sequence/structure/function. Variants that segregated with the observed phenotype were prioritized as follows: stop gain/loss > missense > splice site. Variants with a minor allele frequency greater than 1% were excluded if present in the dbSNP137 (http://www.ncbi.nlm.nih.gov/SNP/) (Sherry et al., 2001), 1000 Genome Project (http://www.1000genomes.org/) (1000 Genomes Project Consortium et al., 2012), Exome Variant Server (Gene ID 7840 (*ALMS1*) and 8291 (*DYSF*) GRCh37; http://evs.gs.washington.edu/EVS/) and The Exome Aggregation Consortium (Version 0.3; http://exac.broadinstitute.org/) databases. PolyPhen2 (Version 2.2.2; http://genetics.bwh.harvard.edu/pph2/) (Adzhubei, et al., 2013), SIFT (last modified August 2011; http://sift.jcvi.org/) (Kumar et al., 2009), Provean (Version 1.1.3; http://provean.jcvi.org/index.php) (Choi et al., 2012), MutationTaster (Build NCBI 37 / Ensembl 69; http://www.mutationtaster.org/) (Schwarz et al., 2010) and VarioWatch (last modified 22 October, 2014; http://genepipe.ncgm.sinica.edu.tw/variowatch/main.do) (Cheng et al., 2012) were used to evaluate the pathogenicity of candidate variants. Integrative Genomics Viewer (Version 2.3.40; https://www.broadinstitute.org/igv/) (Thorvaldsdottir et al., 2013) was used to visualize the sequence position and coverage of candidate variants. Variants of interest were validated using conventional Sanger sequencing. Mutation nomenclature refers to GenBank reference sequence NM_015120.4 for *ALMS1* and NM_003494.3 for *DYSF* (GRCh37). Designations of identified genetic variants follow the guidelines of the Human Genome Variation Society (last modified March 2014; http://www.hgvs.org/mutnome) (den Dunnen and Antonarakis, 2000) and were verified using Mutalyzer (Version 2.0.7; https://mutalyzer.nl/) (Wildeman et al., 2008).

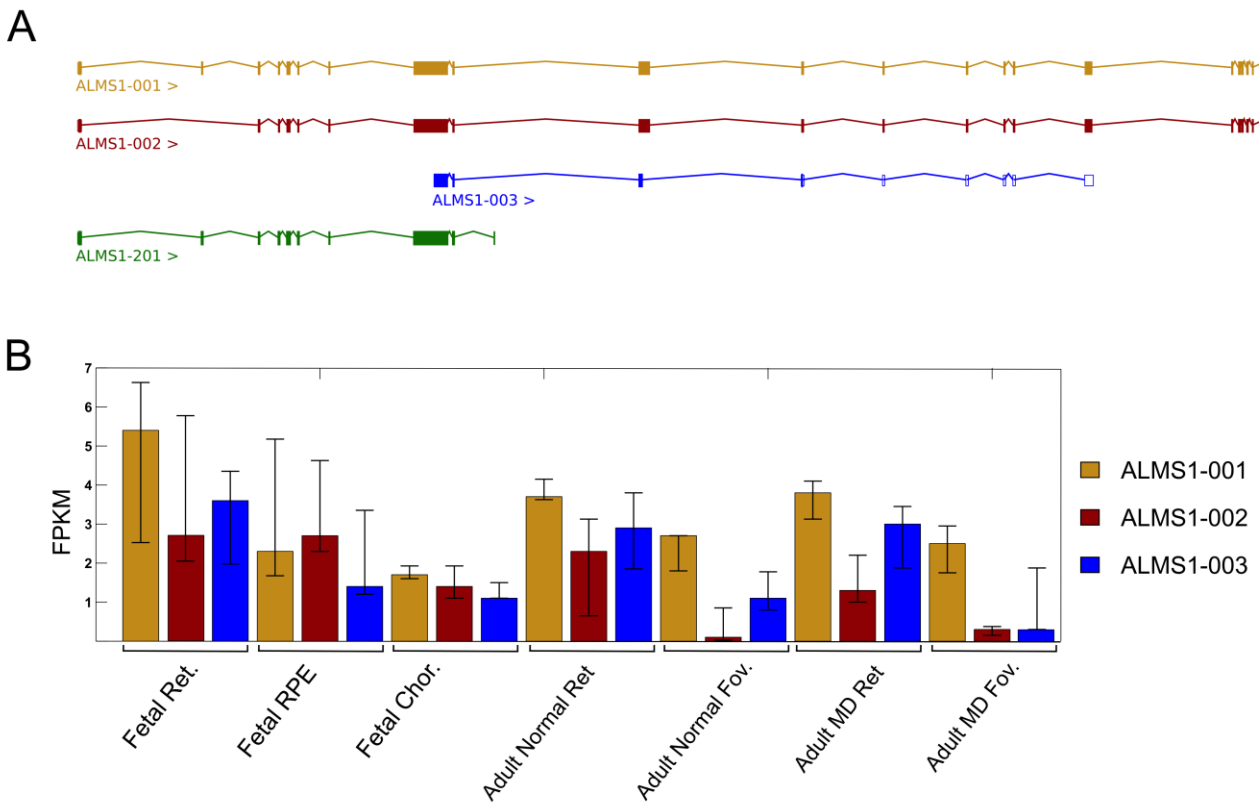

Supp. Figure S1. Human retinal expression data of major *ALMS1* transcripts. The expression of *ALMS1* transcripts was assessed in our in-house retina RNA-seq data obtained after read alignment using Bowtie2 (Langmead and Salzberg, 2012), followed by probabilistic assignment to individual transcripts using eXpress (http://bio.math.berkeley.edu/eXpress/overview.html) expectation maximization algorithm.

(A) Exon structure of human *ALMS1* transcripts (adapted from Ensemble version: ENSG00000116127.13).

(B) Median expression values of *ALMS1* transcripts from fetal and adult retinal tissues, with lower and upper quartiles indicated by error bars. The expression of ALMS1-201 splice variant was absent from all tissues. Ret, retina; RPE, retinal pigment epithelium; Chor, choroid; Fov, fovea; MD, macular degeneration; FPKM, fragments per kilobase of exon per million fragments mapped.

Supp. Table S1. List of identified genetic variants and pathogenicity prediction

Gene (exon)	Nucleotide Change (Protein)	ExAC MAF*	Prediction tools**				
			PolyPhen2 (score)	SIFT (score)	Provean (score)	MutationTaster	VarioWatch
ALMS1 (5)	c.808C>T (p.R270*)	NA	NA	NA	NA	Disease causing automatic	Very high
DYSF (43)	c.4741C>T (p.R1581C)	4.118e-05 (5 het / 121410)	Probably damaging (0.969)	Damaging (0.00)	Deleterious (-7.71)	Disease causing	High
DYSF (55)	c.6209A>G (p.Y2070C)	8.237e-06 (1 het / 121400)	Probably damaging (0.989)	Damaging (0.00)	Deleterious (-5.60)	Disease causing	High

The nucleotide position of each genetic variant was based on the following GenBank cDNA entries (GRCh37): *ALMS1*, NM_015120.4 and *DYSF*, NM_003494.3; Nucleotide numbers reflect cDNA numbering with +1 corresponding to the A of the ATG translation initiation codon in the reference sequence per journal guidelines (www.hgvs.org/mutnomen). The initiation codon is codon 1.

*Broad Institute Exome Aggregation Consortium (ExAC) minor allele frequencies (MAF) are given; in parenthesis, the number of heterozygous (het) alleles observed / total number of individuals is shown; NA, not available.

**Online prediction tools were used to evaluate pathogenicity effects. PolyPhen2 score: >0.909, probably damaging; 0.447 – 0.908, possibly damaging; ≤0.446, benign (Adzhubei et al., 2013). SIFT score: ranges from 0 to1 and represents the probability of the amino acid substitution being damaging (≤0.05) or tolerated (>0.05) (Kumar et al., 2009). Provean score: relative to a predefined threshold (e.g. in our case -2.5) classifies protein sequence variation as deleterious (< -2.5) or neutral (> -2.5) (Choi et al., 2012; http://provean.jcvi.org/index.php). MutationTaster classifies alterations as disease causing (i.e., probably deleterious), disease causing automatic (i.e., known to be deleterious in one of the databases dbSNP, TGP, ClinVar or HGMD), polymorphisms (i.e., probably harmless), polymorphism automatic (i.e., known to be harmless in one of the databases dbSNP, TGP, ClinVar or HGMD). Classifications for each nucleotide position are made by presence of all three possible genotypes in the HapMap data or by presence in TGP (The Gene Partnership) in homozygous state. Alterations that cause a premature termination codon or have <4 homozygous cases in TGP are classified as disease causing. If all three genotypes are present in HapMap data or >4 homozygous cases are present in TGP, the alterations are classified as polymorphisms (http://www.mutationtaster.org/). VarioWatch examines variants within their genomic context, analyzes the functional effect if located in a protein coding region or splice-site, and assigns one of the following risk levels of potential pathogenicity: very high, high, medium, low risk level represented in the decision tree of risk (Cheng et al., 2012).

Supp. Table S2. Clinical ocular findings in patients with *ALMS1* and *DYSF* mutations

Patient Number	Clinical Diagnosis	Visual Acuity (age)	Refraction (age)	LA Cone 30Hz Flicker ERG (age)	DA Rod Response b-wave, µV (age)	DA Mixed Response a/b-wave, µV (age)
MOL0339 III:3	CRD and LGMD2B	0.1 (4,6) 0.05 (9) FC 1m (20) HM (23)	+5 (4) +4 (6) +3 (9)	Impaired cone function flicker NA (10) non-detectable (17)	156 (10) 144 (17)	55 / 176 (10) 66 / 145 (17)
MOL0339 III:4	CRD and LGMD2B	0.1 (3,4) 0.05 (7) FC 1m (14) HM (19)	+1 (3) 0 (4)	Impaired cone function flicker NA (8) non-detectable(14)	156 (8) NA (14)	56 / 244 (8) 126 / 97 (14) negative pattern

- CRD, cone-rod dystrophy; LGMD2B, limb-girdle muscular dystrophy type 2B;
- Data represent average between both eyes;
- Best corrected visual acuity given as ratio; when below 0.05, Finger Counting (FC) is provided in meters, Hand Movements (HM);
- Refraction, given as mean spherical equivalent of both eyes, in diopters;
- Full-field Electroretinography (ERG) results include the following details: Light-adapted (LA) cone flicker amplitude (normal 60–144 µV) and implicit time (IT, in ms, normal 27–33 ms); Dark-adapted (DA) rod response b-wave amplitude (normal range 200–500 µV); Dark-adapted mixed cone-rod a- and b-wave amplitudes (normal a-wave 90–350 µV, normal b-wave 380–630 µV). NA, not available. In both patients, the early ERG recording at age 10 (III:3) and age 8 (III:4) were difficult to perform and assess because of low compliance, marked Bell's phenomenon and nystagmus; consequently, high levels of background noise were present.

Supp. Table S3. List of clinical features of Alström syndrome examined in the patients

Clinical Features	**Patients III:3 and III:4**
Vision	Cone-Rod dystrophy, nystagmus, photophobia, low visual acuity
Hearing	WNL
Heart function	WNL
Hypertension	No
Diabetes Mellitus	No
Cholesterol and triglyceride levels	WNL
Liver function tests	Mildly impaired (as detailed in text)
Thyroid function	WNL
Gastrointestinal problems (reflux, etc)	None
Hypogonadism	No
Short stature, Scoliosis, Skeletal abnormalities	None
Urological symptoms	None
Pulmonary symptoms	None
Neurological signs	None
Birth problems	No
Chronic otitis media	No
Developmental delay	No (only difficulties secondary to low vision; both successfully completed high school, and one studied in the university)
Other unusual features	Muscular dystrophy (secondary to Dysferlin mutation)

Throughout the years, both siblings were examined several times by ophthalmologists, pediatricians, neurologists and genetic counselors. WNL, within normal limits.

Supp. References

1000 Genomes Project Consortium, Abecasis GR, Auton A, Brooks LD, DePristo MA, Durcin RM, Handsaker RE, Kang HM, Marth GT, McVean GA. 2012. An integrated map of genetic variation from 1,092 human genomes. Nature 491: 56-65.

Adzhubei I, Jordan DM, Sunyaev SR. 2013. Predicting functional effect of human missense mutations using PolyPhen-2. Curr Protoc in Hum Genet 76:7.20:7.20.1-7.20.41.

Cheng YC, Hsiao FC, Yeh EC, Lin WJ, Tang CY, Tseng HC, Wu HT, Liu CK, Chen CC, Chen YT, Yao A. 2012. VarioWatch: providing large-scale and comprehensive annotations on human genomic variants in the next generation sequencing era. Nucleic Acid Res 40:W76-81.

Choi Y, Sims GE, Murphy S, Miller JR, Chan AP. 2012. Predicting the functional effect of amino acid substitutions and indels. PloS One 7:e46688.

den Dunnen JT, Antonarakis SE. 2000. Mutation nomenclature extensions and suggestions to describe complex mutations: a discussion. Hum Mutat 15:7-12.

Kumar P, Henikoff S, Ng PC. 2009. Predicting the effects of coding non-synonymous variants on protein function using the SIFT algorithm. Nat Protoc 4:1073-81.

Langmead B, Salzberg SL. 2012. Fast gapped-read alignment with Bowtie 2. Nat Methods 9:357-9.

Li H, Handsaker B, Wysoker A, Fennell T, Ruan J, Homer N, Marth G, Abecasis G, Durbin R, Genome Project Data Processing Subgroup. 2009. The Sequence Alignment/Map format and SAMtools. Bioinformatics 25:2078-9.

Schwarz JM, Rodelsperger C, Schuelke M, Seelow D. 2010. MutationTaster evaluates disease-causing potential of sequence alterations. Nat Methods 7:575-6.

Seelow D, Schuelke M, Hildebrandt F, Numberg P. 2009. HomozygosityMapper--an interactive approach to homozygosity mapping. Nucleic Acids Res 37:W593-99.

Sherry ST, Ward MH, Kholodov M, Baker J, Phan L, Smigielski EM, Sirotkin K. 2001, dbSNP: the NCBI database of genetic variation. Nucleic Acids Res 29:308-11.

Thorvaldsdottir H, Robinson JT, Mesirov JP. 2013. Integrative Genomics Viewer (IGV): high-performance genomics data visualization and exploration. Brief Bioinform 14:178-92.

Wang K, Li M, Hakonarson H. 2010. ANNOVAR: functional annotation of genetic variants from high-throughput sequencing data. Nucleic Acids Res 38:e164.

Wildeman M, van Ophuizen E, den Dunnen JT, Taschner PE. 2008. Improving sequence variant descriptions in mutation databases and literature using the Mutalyzer sequence variation nomenclature checker. Hum Mutat 29:6-13.